Preprints.org

Article

Not peer-reviewed version

Precise Detection and Transcriptomic Concordant Analysis of Circulating Tumor Cells from Prostate Cancer

Hyungseok Cho , Ki-Ho Han * , Jae-Seung Chung * , Seok-Soo Byun , Jae Il Chung , Won Ik Seo , Chan Ho Lee

Posted Date: 27 October 2023

doi: 10.20944/preprints202310.1760.v1

Keywords: prostate cancer; circulating tumor cells; lateral magnetophoresis; prostate-specific antigen; prostate-specific membrane antigen; biomarker; liquid biopsy

Preprints.org is a free multidiscipline platform providing preprint service that is dedicated to making early versions of research outputs permanently available and citable. Preprints posted at Preprints.org appear in Web of Science, Crossref, Google Scholar, Scilit, Europe PMC.

Copyright: This is an open access article distributed under the Creative Commons Attribution License which permits unrestricted use, distribution, and reproduction in any medium, provided the original work is properly cited.

Preprints (www.preprints.org) | NOT PEER-REVIEWED | Posted: 27 October 2023 doi:10.20944/preprints202310.1760.v1

Disclaimer/Publisher's Note: The statements, opinions, and data contained in all publications are solely those of the individual author(s) and contributor(s) and not of MDPI and/or the editor(s). MDPI and/or the editor(s) disclaim responsibility for any injury to people or property resulting from any ideas, methods, instructions, or products referred to in the content.

Article

Precise Detection and Transcriptomic Concordant Analysis of Circulating Tumor Cells from Prostate Cancer

Hyungseok Cho [1], Ki-Ho Han [1,*], Jae-Seung Chung [3,*], Seok-Soo Byun [2], Jae Il Chung [4], Won Ik Seo [4] and Chan Ho Lee [4]

[1] Department of Nanoscience and Engineering Center for Nano Manufacturing, Inje University, Gimhae, Republic of Korea; biomems@inje.ac.kr (H.C.)
[2] Department of Urology, Seoul National University Bundang Hospital, Seongnam, Republic of Korea
[3] Department of Urology, Haeundae Paik Hospital, Inje University College of Medicine, Busan, Republic of Korea
[4] Department of Urology, Busan Paik Hospital, Inje University College of Medicine, Busan, Republic of Korea
* Correspondence: mems@inje.ac.kr (K.-H.H.); biogen@hanmail.net (J.-S.C.); Tel.: +82-55-320-3715 (K.-H. H.); +82-51-797-2260 (J.-S.C.)

Abstract: This study focused on the precise detection and concordant analysis of circulating tumor cells (CTCs) to verify the usefulness of CTCs as promising clinical markers. CTCs are traditionally achieved using immune-fluorescence and morphological techniques. By combining two prostate cancer-specific genes (PSA and PSMA) and two epithelial-specific genes (EpCAM and KRT19), the CTC detection efficiency can be enhanced. The detection rates of localized prostate cancer (LPC), locally advanced prostate cancer (LAPC), metastatic hormone-sensitive prostate cancer (mHSPC), and metastatic castration-resistive prostate cancer (mCRPC) were 63.04 % (29/46), 70.59% (34/51), 94.34% (50/53), and 90% (126/140), respectively. Subsequent correlation analysis between the four genes, baseline PSA, and CTC count revealed that only the CTC count correlated with baseline PSA in the localized stages of prostate cancer, whereas all four genes were correlated with baseline PSA and CTC count in the metastatic stages of prostate cancer. The precise detection of CTCs using both numerical and transcriptomic analyses can improve the accuracy of biomarker investigations. This study provides valuable insights into the limitations of serum PSA testing and offers a promising alternative to diagnose and manage prostate cancer via the CTC number and specific genes for prostate cancer.

Keywords: prostate cancer; circulating tumor cells; lateral magnetophoresis; prostate-specific antigen; prostate-specific membrane antigen; biomarker; liquid biopsy

1. Introduction

Serum prostate-specific antigen (sPSA), a standardized diagnostic/prognostic marker for prostate cancer (PC), is widely used for real-time monitoring of patient status and provides guidance for the clinical management of PC. Although sPSA is conventionally used as a prostate marker, the low specificity and sensitivity of sPSA tests may lead to the overdiagnosis of PC and uncertainty regarding a patient's cancer status [1–3]. Therefore, the use of liquid biopsy-based biomarkers, including circulating tumor cells (CTCs), exosomes, and circulating nucleic acids (ctDNA and ctRNA), has been proposed.

CTCs are considered surrogate and predictive markers as they have two distinguishable features: the isolated number (CTC#) and the genomic materials [4,5]. The exact pattern of isolated CTCs and their genomic expression during cancer stages are essential for precise diagnoses and prognoses in cancer management. Furthermore, CTCs should reflect the patient's clinical status at the time of blood sampling [6]. For clinical usability, the CTC# and genomic materials should be compared or validated using standardized clinical markers such as sPSA levels, Gleason score (GS), bone scan index, alkaline phosphatase levels, and lactase dehydrogenase levels [6–8].

© 2023 by the author(s). Distributed under a Creative Commons CC BY license.

Preprints (www.preprints.org) | NOT PEER-REVIEWED | Posted: 27 October 2023 doi:10.20944/preprints202310.1760.v1

In the basic hypothesis, a reduction in tumor size is mirrored by decreased sPSA levels and growing tumors are detected by increased sPSA levels [3,9]. Cancer-related genomic materials can spread into the blood circulation depending on the tumor's aggressiveness during the primary/metastatic stages [10–12]. The CTC# may increase in a dose-dependent manner based on changes in cancer progression and clinical stage. The CTC# is correlated with the upregulation of cancer-associated genes [13]. However, the relationship between the CTC# and gene expression in different prostate cancer stages remains unclear.

Several studies have reported that an increased CTC# is related to overall survival and biochemical recurrence (BCR) in patients with PC [14–17]. Baseline CTC# have been compared with sPSA levels to verify the use of CTC features to predict survival, risks, and metastasis using the US Food and Drug Administration-approved CTC assay Cellsearch (MENARINI Silicon Biosystems, Italy) [7,8,18,19]. However, the CTC# was not associated with clinical status or cancer stage in a previous study [20], and CTCs were not detectable during the early stages of PC [21] due to the low detection rate, limiting its clinical usefulness. Furthermore, the concordance analysis did not show the same tendencies across all stages of PC.

The genomic approach is based on the transcriptomic abundance of sPSA [22,23], prostate-specific membrane antigen (PSMA) [19,24,25], prostate stem cell antigen [26], as well as various gene combinations [27] that are measured using real-time polymerase chain reaction (RT-PCR). Although reasonable clinical signatures have been identified, this method is limited clinically by its low sensitivity and specificity [22,24,28]. The genomic detection-based assay AdnaTest (QIAGEN, Germany) was developed using mRNA-PSA, PSMA, and EGFR genes. Although gene-based approaches demonstrate clinically meaningful results [29], this method is hard to reflect whole characteristics of patients because of exception in CTC# [30]. Therefore, the use of the co-analytical approach to characterize the CTC tendencies at different clinical stages using genomic patterns remains controversial. In addition, several studies have reported correlations between clinical outcomes and CTC# in patients with PC [31,32], though there is a lack of studies regarding the relationship of CTC# and mRNA-based transcriptomic levels at specific biopsy time points. The CTC# in patients with metastasis is crucial for cancer management when combined with sPSA level as radical clinical changes occur in these patients as the disease progresses [4,7]. Therefore, the correlations between the CTC# isolated and pathological stages of PC have not yet been clearly identified. In addition, the correlation of cancer-related mRNA expression levels in CTCs and with the CTC# and sPSA levels remains unclear. Consequently, the precise CTC# should be analyzed in concordance with genomic information for each stage of prostate cancer compared with standardized clinical markers. To derive accurate clinical results using CTCs, precision isolation techniques that can separate precise and sufficient quantities of CTCs are needed. After separation, it is essential to accurately determine the presence or absence of CTCs as CTC detection is not precise when conventional imaging techniques are used. These limitations can be effectively addressed by detecting genes specific to both PC and CTCs.

This study reports a sensitive and highly reproducible CTC isolation technology based on lateral magnetophoresis using a microfluidic manufacturing process. This demonstrates the isolation efficiency and clinical utility in patients with breast [33], pancreatic [34,35], and prostate cancer [30,34,36,37] using information regarding the CTC# and the genomic analysis of CTC genes. In this study, we analyzed the precise CTC detection rates of four transcriptomic genes derived from CTCs: mRNA-based PSA and PSMA for prostate cancer, and EpCAM and KRT19 for epithelial-specific genes, using conventional imaging techniques. Then, a concordance analysis assessing the baseline sPSA concentration, CTC#, and four transcriptomic genes was subsequently conducted to investigate the clinical role of CTCs as a surrogate biomarker in patients with PC.

Preprints (www.preprints.org) | NOT PEER-REVIEWED | Posted: 27 October 2023 doi:10.20944/preprints202310.1760.v1

2. Materials and Methods

2.1. Patients

Blood samples from patients with localized prostate cancer (LPC) (n=46), locally advanced prostate cancer (LAPC) (n=51), metastatic hormone-sensitive prostate cancer (mHSPC) (n=53), and metastatic castration-resistant prostate cancer (mCRPC) (n=140) were used in the current study (Table 1). Samples from healthy donor (HD) (n=9) and patients with benign prostatic hyperplasia (BPH) (n = 21) were also included. All patients provided written informed consent and the study was approved by the appropriate institutional review boards.

Table 1. Characteristics and clinical features of the recruited prostate cancer patients.

	Localized stage		**Metastatic stage**	
	LPC (n=46)	**LAPC (n=51)**	**mHSPC (n=53)**	**mCRPC (n=140)**
Age, median, IQR, years	69.1 (54-83)	73.1 (59-86)	73.7 (56-87)	74.2 (50-86)
PSA, median, IQR, ng/ml	8.0 (1.91-22.8)	39.1 (0.01-168)	504.3 (0.05-5000)	187.9 (0.01-2787)
Gleason Score (%)				
6	60.9	7.8	7.5	0.7
7	28.2	27.5	17.0	10.0
≥ 8	10.9	60.8	75.5	83.6

2.2. Sample preparation

To enhance the isolation efficiency, red blood cells (RBCs) were initially separated via density gradient centrifugation at 700 × g for 30 min in Ficoll solution (1.119 g/mL, Histopaque-1119, Sigma-Aldrich). The resulting buffy coat layer was collected and introduced into 10 mL of ice-cold phosphate-buffered saline (PBS; GenDEPOT) containing 0.2% bovine serum albumin (BSA; AMRESCO). Subsequently, the nucleated cells were resuspended in 200 μL of ice-cold PBS with 0.2% BSA inside a 1.5-mL microcentrifuge tube. After cleansing, the nucleated cells were resuspended in 200 μL of the ice-cold PBS-BSA solution. Antibodies targeting EpCAM and magnetic nanobeads were added and the samples incubated at 4°C for 60 and 90 minutes, respectively (Figure 1a). The final suspension was adjusted to a volume of 1 mL using 800 μL of the ice-cold PBS solution containing 0.2% BSA.

2.3. CTC isolation

The CTCs were separated using a disposable CTC microseparator (CTC-dμChip) with lateral magnetophoretic technology. This device consists of a disposable microchannel designed for single-use applications and a reusable wire substrate that simply assembled using vacuum application (Figure 1b). The prepared sample was injected into the sample inlet of the chip as the buffer solution was introduced into the buffer inlet at flow rates of 2 ml/h. The separation process typically occurred within 30 min. Upon injection, the CTCs specifically bound to the EpCAM antibody and immunomagnetic beads immediately encountered the first ferromagnetic wire and were pulled downward. Subsequently, lateral fluidic forces flowing in the direction of the fluid velocity pushed the CTCs toward another ferromagnetic wire that pulled the cells downward. Ultimately, the CTCs were separated and exited through the CTC outlet located at the bottom of the chip. The separated CTCs were used for the subsequent count analysis and mRNA gene analysis (Figure 1c). Each blood sample was separated into two equal halves that were used for the CTC# analysis and mRNA-gene detection. The detailed device fabrication and working principle with analytical results have been reported previously [33,36].

Preprints (www.preprints.org) | NOT PEER-REVIEWED | Posted: 27 October 2023 doi:10.20944/preprints202310.1760.v1

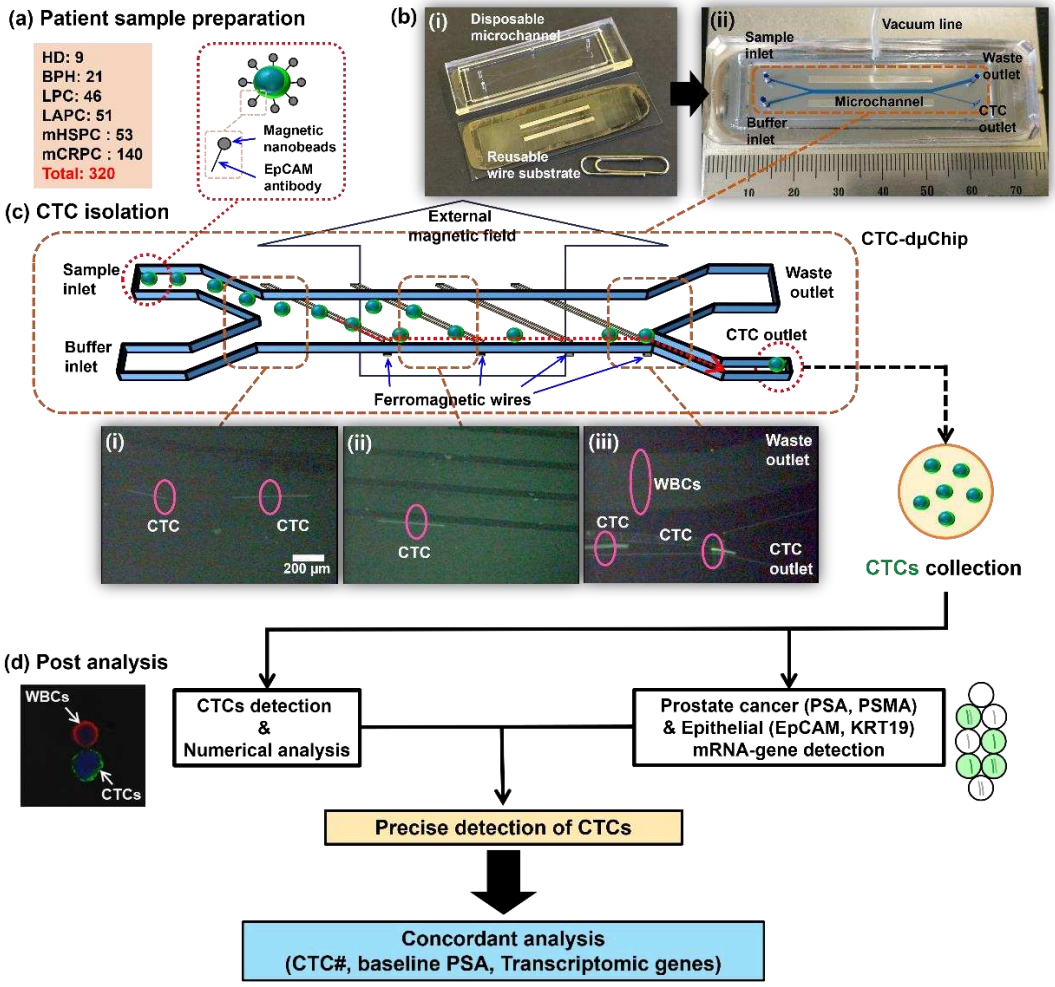

Figure 1. Overview of the experimental workflow. (a) Samples were provided from patients in control groups (HD, n=9; BPH, n=21) and prostate cancer groups (LPC, n=46; LAPC, n=51; mHSPC, n=53; mCRPC, n=140) and labeled with the EpCAM antigen and immunomagnetic nanobeads. (b) A disposable CTC microseparator (CTC-dμChip) showing (i) the disposable microchannel with reusable wire substrate and (ii) assembly via a vacuum system are shown. (c) The working principle of CTC isolation is presented: (i) Injected CTCs from the sample inlet, (ii) laterally isolated CTCs in the microchannel center, and (iii) final CTC isolation at the CTC outlet. (d) Analysis of isolated CTCs: Half of the patient's blood was used for CTC detection using the immune-fluorescence method while the remaining half was used for transcriptomic detection via the ddPCR method. The precise identification of CTCs integrated both numerical and mRNA-gene detections. Subsequent correlation analyses considered three factors: CTC#, baseline PSA, and mRNA-genes. Abbreviations: *circulating tumor cells (CTCs), white blood cells (WBCs), healthy donor (HD), benign prostatic hyperplasia (BPH), localized prostate cancer (LPC), locally advanced prostate cancer (LAPC), metastatic hormone-sensitive prostate cancer (mHSPC), metastatic castration-resistive prostate cancer (mCRPC), prostate cancer (PC), epithelial cell adhesion molecules (EpCAM), cytokeratin 19 (KRT19), prostate specific antigen (PSA), prostate specific membrane antigen (PSMA).*

2.4. CTC enumeration

The samples containing CTC and co-isolated white blood cells (WBCs) were fixed with 100 μL of 4% paraformaldehyde during a 10-min incubation. For nuclei labeling, 20 μL of DAPI (Invitrogen) was used. Concurrently, WBCs were distinctly labeled using 2.5 μL of Alexa Fluor 647 antibodies (Biolegend) against CD45 after a 30-min incubation at 4°C. To permeabilize the cell membranes, 200 μL of 0.2% Triton X-100 (AMRESCO) was applied for 5 min under room conditions. The CTCs were stained using 0.3 μL of Alexa Fluor 488 antibodies targeting pan-cytokeratin (eBioscience). Following

Preprints (www.preprints.org) | NOT PEER-REVIEWED | Posted: 27 October 2023 doi:10.20944/preprints202310.1760.v1

immune-fluorescence staining, the CTCs and WBCs were counted using a confocal microscope (LSM800, Carl Zeiss) (Figure 1d and Figure 2). The counts were normalized based on the blood volume used, resulting in a representation of cells/mL for easier comparative analyses. The optimal cutoff value for the detection rate was 2.1 CTCs/mL, which was set based on the highest CTC count of the HD samples. The purity rate of the isolated CTCs was calculated as the ratio of CTCs to the total number of enumerated nucleated cells (CTCs/CTCs+WBCs).

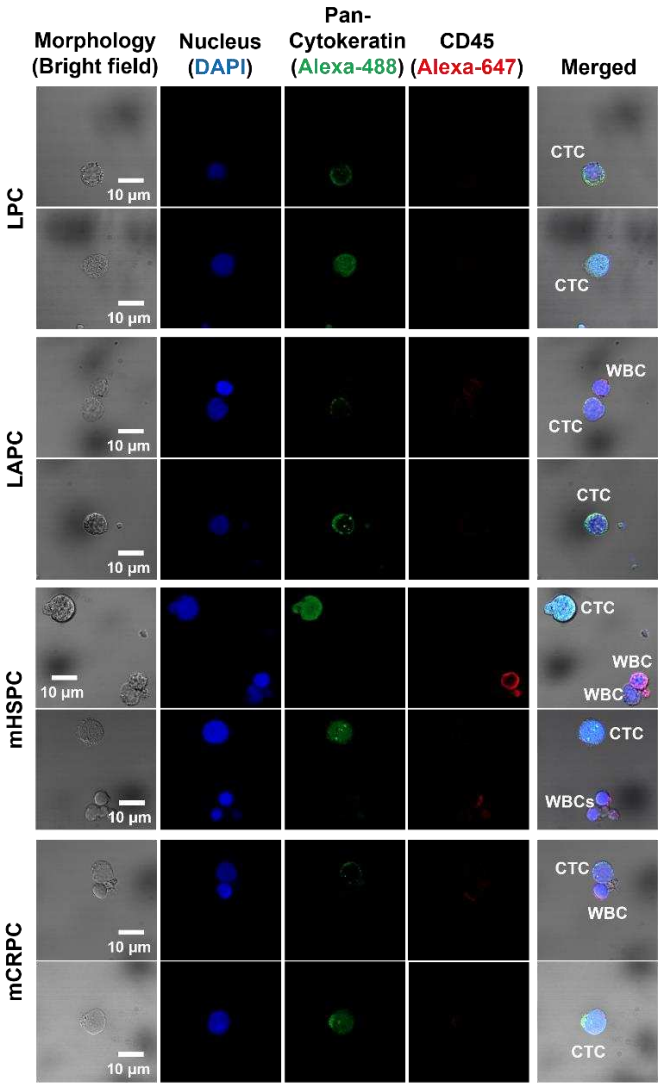

Figure 2. Isolated CTCs. Circulating tumor cells (CTCs) derived from patients with prostate cancer are categorized by their respective clinical stages: LPC, LAPC, mHSPC and mCRPC (Scale bar: 10 μm). Abbreviations: localized prostate cancer (LPC), locally advanced prostate cancer (LAPC), metastatic hormone-sensitive prostate cancer (mHSPC), metastatic castration-resistive prostate cancer (mCRPC).

2.5. Transcriptomic detection

mRNA-PSA, PSMA, mRNA-EpCAM, and KRT19 were detected in the CTC samples (Figure 1d). mRNA-GAPDH was used as the housekeeping gene, and mRNA-CD45 as the leukocyte-specific control gene. The mRNA was extracted, followed by cDNA synthesis (Supplementary S1), and a pre-amplification process to enhance detection efficiency (Supplementary S2). The amplified template underwent droplet digital PCR (ddPCR; QX200, Bio-Rad) for final gene detection (Supplementary S3). The primer sequences and product sizes for the four genes are listed in Table S1. The cutoff values for each gene were determined previously [36]. Each cut-off value was increased by 0.001 copies/μL for log-scale transformation. To ensure accurate genomic analyses, the detection thresholds were 0.12

Preprints (www.preprints.org) | NOT PEER-REVIEWED | Posted: 27 October 2023 doi:10.20944/preprints202310.1760.v1

copies/μL for PSA, 0.22 copies/μL for PSMA, 0.29 copies/μL for EpCAM and 0.12 copies/μL for KRT19 determined based on the maximum values that were measured in no-template control samples [36].

2.6. CTC detection criteria

The precise detection of CTCs was confirmed using a numerical analysis based on immune-fluorescence with a morphology analysis conducted using a confocal microscope. If one of the two epithelial genes (EpCAM and KRT19) is detected and, concurrently, one of the two prostate cancer-specific genes (PSA and PSMA) is detected, it was considered that CTCs are present. In other words, at least one of each type of gene must be detected simultaneously for the sample to be considered as having CTCs even if CTCs were not detected during the numerical analysis. The final detection rate was derived from the sum of the detection rates obtained via the numerical and mRNA-gene analyses (Figure 1d).

2.7. Statistical analysis

Pearson's correlation coefficient was calculated using OriginPro (version 2023b; OriginLab). All statistical analyses were performed using SPSS (version 24.0). Statistical significance was set at $p < 0.05$. All graphs and heat maps were created using OriginPro 2023b (OriginLab) and Excel (Microsoft).

3. Results

3.1. Numerical analysis

The number of CTCs isolated increased as the clinical stage of the disease progressed (Figures 3a-b). The number of CTCs was normalized per mL of blood. The threshold value of CTC# was set at 2.1 CTCs/mL, which is 0.1 CTCs/mL above the highest CTC# isolated from healthy donors (Figure 3c). The average CTC# was 0.58 CTCs/mL in the HD samples, 0.93 CTCs/mL in the BPH samples, 2.11 CTCs/mL in the LPC samples, 4.90 CTCs/mL in the LAPC samples, 10.66 CTCs/mL in the mHSPC samples, and 15.97 CTCs/mL in the mCRPC samples (Figure 3c). Based on the cutoff value, the detection rate of CTCs was 14.29% (3/21) in the BPH samples, 47.83% (22/46) in the LPC samples, 62.75% (32/51) in the LAPC samples, 83.02% (44/53) in the mHSPC samples, and 85.71% (120/140) in the mCRPC samples (Figure 3d). The average purity rates of the BPH, LPC, LAPC, mHSPC, and mCRPC samples were 0.36%, 0.91%, 1.73%, 2.47%, and 3.17%, respectively (Figure 3e). The CTC#, CTC detection rate, and CTC purity rate increased as the clinical stage of disease progressed.

Preprints (www.preprints.org) | NOT PEER-REVIEWED | Posted: 27 October 2023 doi:10.20944/preprints202310.1760.v1

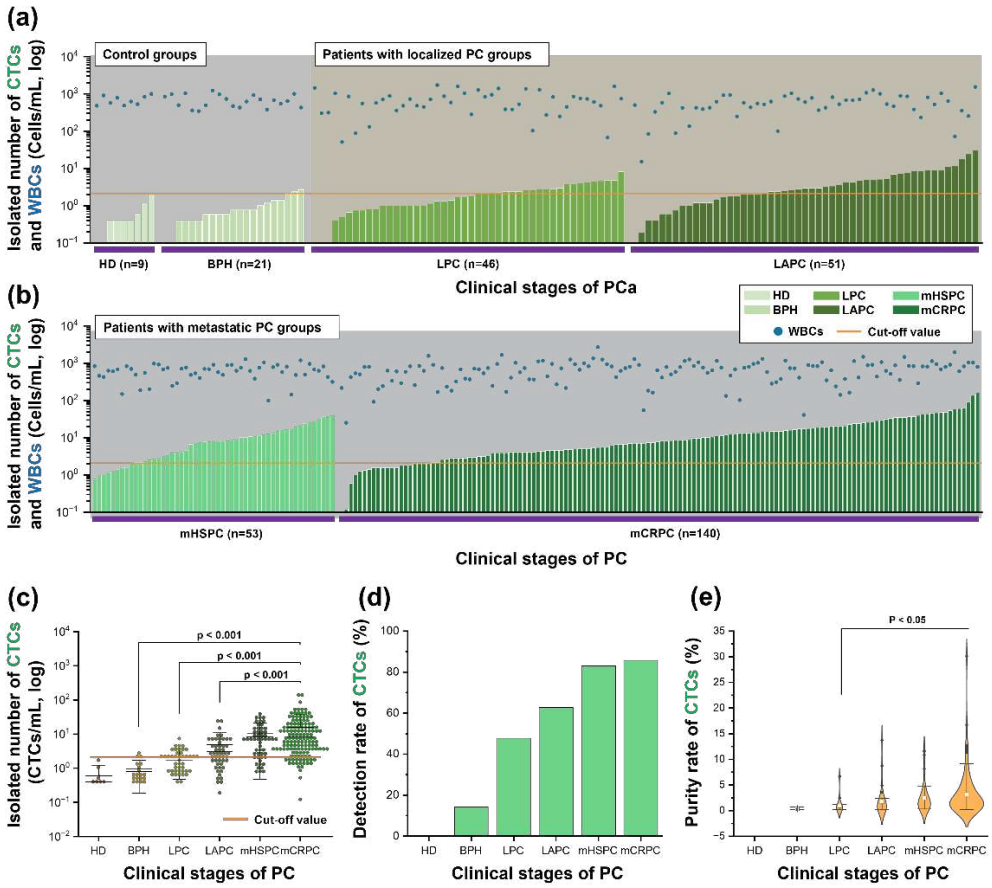

Figure 3. Numerical results of isolated CTCs. (a) The CTC# and the co-isolated white blood cell (WBC) counts are shown for the control groups, HD and BPH, and patients diagnosed with localized and locally advanced prostate cancer. (b) A detailed representation of the CTC# and co-isolated WBC count from patients with metastatic prostate cancer stages, including mHSPC and mCRPC is shown. (c) The CTC# detection threshold is set at 2.1 CTCs/mL. (d) The rate of CTC detection achieved using the immune-fluorescence method is shown for different clinical states of PC. (e) The purity rate of the isolated CTCs showed an upward trend as the clinical stages of prostate cancer progress. Abbreviations: circulating tumor cells (CTCs), white blood cells (WBCs), healthy donor (HD), benign prostatic hyperplasia (BPH), localized prostate cancer (LPC), locally advanced prostate cancer (LAPC), metastatic hormone-sensitive prostate cancer (mHSPC), metastatic castration-resistive prostate cancer (mCRPC), prostate cancer (PC).

3.2. Transcriptosome analysis

The expressions of mRNA-PSA, PSMA, EpCAM, and KRT19 genes were not detected in one BPH sample and one mHSPC sample due to poor sample quality or technical issues. The threshold value of each gene was determined (Figure 4).

The mean expression and the detection rate of PSA-mRNA were 0.08 copies/μL and 15% (3/20) in BPH samples; 0.06 copies/μL and 13.04% (6/46) in LPC samples; 0.07 copies/μL and 15.69% (8/51) in LAPC samples; 7229.58 copies/μL and 61.54% (32/52) in mHSPC samples; and 4970.53 copies/μL and 63.57% (89/140) in mCRPC samples (Figure 4a and 4b). The expression level of PSA mRNA was significantly higher in the metastatic stages of PC than in the localized stages ($p<0.01$). As shown in Figure 4c, PSMA-mRNA exhibited a similar expression pattern as PSA-mRNA. The mean expression and detection rate of PSMA-mRNA were 2.51 copies/μL and 15% (3/20) in BPH samples; 1.30 copies/μL and 30.43% (14/46) in LPC samples; 0.511 copies/μL and 43.14% in LAPC samples; 21828.14 copies/μL and 63.46% (33/52) in mHSPC samples; and 1512.08 copies/μL and 60% (84/140) in mCRPC samples (Figures 4c and 4d). The mHSPC samples had the highest expression of PSMA-mRNA. The detection rate of PSMA mRNA was higher than that of PSA-mRNA in LPC and LAPC samples.

Preprints (www.preprints.org) | NOT PEER-REVIEWED | Posted: 27 October 2023 doi:10.20944/preprints202310.1760.v1

The mean expression and detection rate of EpCAM-mRNA were 22.24 copies/μL and 44.44% (4/9) in HD samples; 16.73 copies/μL and 55% (11/20) in BPH samples; 108.88 copies/μL and 56.52% (26/46) in LPC samples; 11.04 copies/μL and 68.63% (35/51) in LAPCsamples; 640.21 copies/μL and 71.15% (37/52) in mHSPC samples; and 303.77 copies/μL and 72.86% (102/140) in mCRPC samples (Figure 4e and 4f). The mean expression and detection rates of KRT19-mRNA were 333.38 copies/μL and 22.22% (2/9) in HD samples; 7.34 copies/μL and 45% (9/20) in BPH samples; 0.76 copies/μL and 28.26% (13/46) in LPC samples; 0.59 copies/μL and 27.45% (14/51) in LAPC samples; 21671.90 copies/μL and 65.38% (34/52) in mHSPC samples; and 1245.29 copies/μL and 65% (91/140) in mCRPC samples (Figure 4g and 4h). The pattern of KRT19-mRNA mRNA detection was similar to those of mRNA-PSA and PSMA, including overexpression in the metastatic samples.

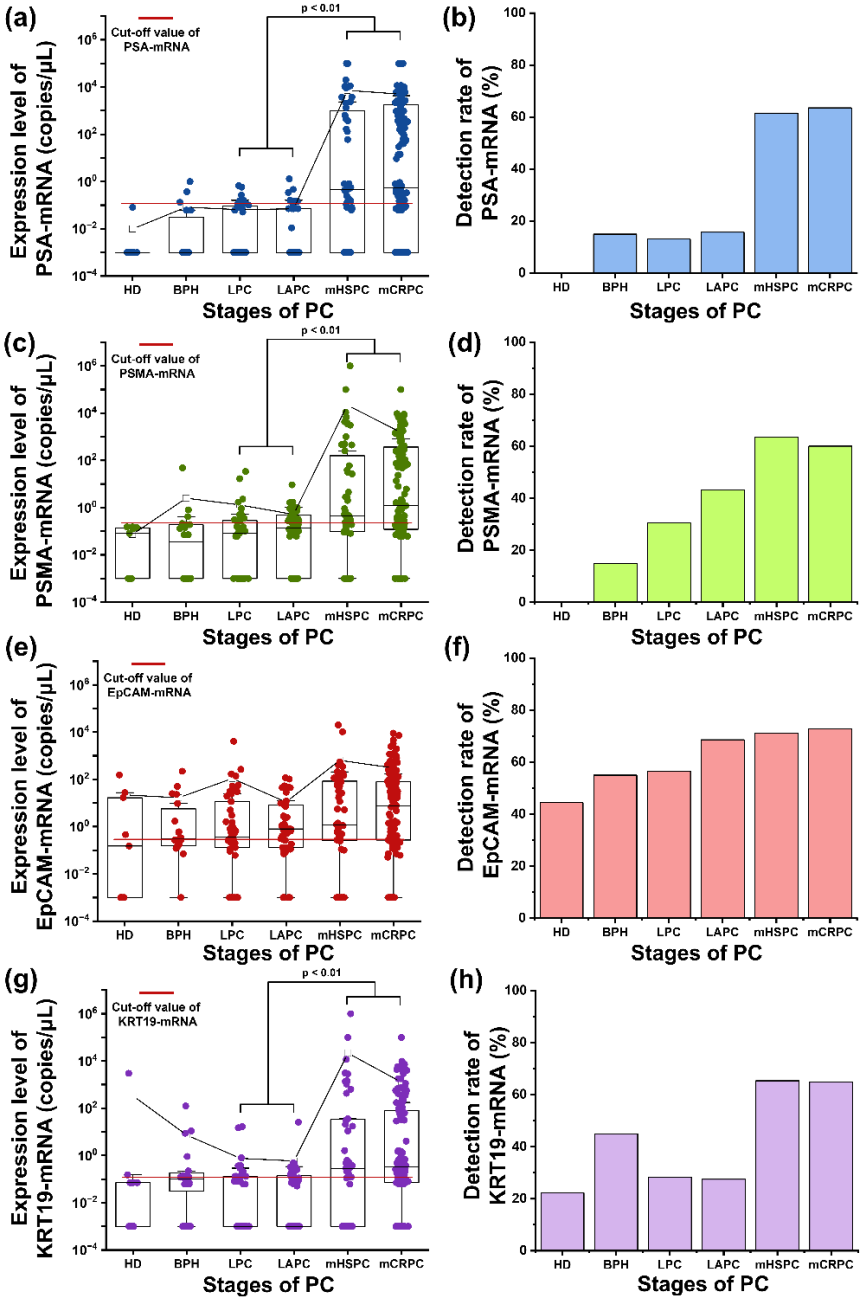

Figure 4. Expression level of genes and detection rate. (a) The expressions of PSA-mRNA are shown in patients with different stages of PC. (b) PSA-mRNA was detected at a threshold of 0.12 copies/μL. (c) The PSMA-mRNA expressions of each sample group are shown. (d) The detection rate of PSMA-mRNA is shown, using a specific cut-off value of 0.22 copies/μL to determine the relevant expression

Preprints (www.preprints.org) | NOT PEER-REVIEWED | Posted: 27 October 2023 doi:10.20944/preprints202310.1760.v1

levels. (e) The expression of EpCAM-mRNA shows its relative abundance in the sample groups. (f) A threshold of 0.29 copies/μL EpCAM-mRNA is used to show significant detection levels. (g) The expression dynamics of KRT19-mRNA are illustrated, focusing on its distribution during the stages of prostate cancer. (h) The detection rate for KRT19-mRNA is shown. A cut-off value of 0.12 copies/μL was used. Abbreviation: healthy donor (HD), benign prostatic hyperplasia (BPH), localized prostate cancer (LPC), locally advanced prostate cancer (LAPC), metastatic hormone-sensitive prostate cancer (mHSPC), metastatic castration-resistive prostate cancer (mCRPC), prostate cancer (PC), epithelial cell adhesion molecules (EpCAM), cytokeratin 19 (KRT19), prostate specific antigen (PSA), prostate specific membrane antigen (PSMA).

3.3. Precise detection of CTCs

In LAPC, as the baseline PSA levels increase, there is a tendency for the number of CTCs to increase, but the trends in gene expression are not distinctly visible (Figure 5a(i)-(iii). However, in the metastatic groups, as the baseline PSA levels increase, the expression of the genes displayed on the heatmap shows an increasing pattern, and increasing tendency observed in the number of CTCs in mHSPC rather than mCRPC (Figure 5b(i)-(iii)). In addition, When CTCs were not detected, they were frequently identified in localized PC group samples using transcriptomic detection methods. But significant CTC# were already detected in the metastatic PC groups using a numerical analysis (Figure 5a(iv) and 5b(iv)). Therefore, the transcriptomic detection method did not substantially affect this stage. However, the CTC detection rate was low in localized PC groups, and the transcriptomic detection method can be used to localized PC group to increasing the detection rate.

The final detection rates of CTCs were 28.57% (3+3/21) in BPH samples; 63.04% (22+7/46) in LPC samples; 70.59% (32+4/51) in LAPC samples; 94.34% (44+6/53) in mHSPC samples; and 90% (120+6/140) in mCRPC samples (Figure 5c).

3.4. Correlative analysis

In a comprehensive scatter plot representation, mRNA-genes were showcased using combined morphological and genomic positive samples. Following this, Pearson's correlation was derived through linear regression analysis. Primarily, genes specific to prostate cancer were discerned for their correlation with baseline PSA concentrations and CTC#. Figures 6(a) and 6(b) displayed the relationship between PSA-mRNA and PSMA-mRNA genes vis-à-vis the baseline PSA concentration. Interestingly, some mCRPC samples denoted minute transcriptomic concentrations (0.001 copies/μL), yet the correlations for both genes remained significant: PSA-mRNA [mHSPC: R=0.486 ($p<0.001$); mCRPC: R=0.656 ($p<0.001$) in Figure 6(a)] and PSMA-mRNA [mHSPC: R=0.528 ($p<0.001$); mCRPC: R=0.533 ($p<0.001$) in Figure 6(b)]. CTC# correlations to baseline PSA concentration were elucidated in Figure 6(c), wherein LPC and LAPC stages exhibited associations [LPC: R=0.419 ($p=0.023$); LAPCa: R=0.551 ($p<0.001$)], mirroring our previous research outcomes. Notably, in the CTC# analysis, the mHSPC stage manifested the most potent correlation with baseline PSA concentrations [R=0.669 ($p<0.001$)], indicating potential sample size nuances. Furthermore, a pronounced correlation was discerned between PSA-mRNA and PSMA-mRNA [mHSPC: R=0.676 ($p<0.001$); mCRPC: R=0.749 ($p<0.001$)] as depicted in Figure 6(d). These findings align cohesively with gene expression patterns observed in Figures 4(a) and 4(c). Figures 6(e) and 6(f) present correlations between the mentioned genes and CTC#, demonstrating robust correlations in mHSPC [PSA-mRNA: R=0.576 ($p<0.001$); PSMA-mRNA: R=0.554 ($p<0.001$)] and moderate associations in mCRPC [PSA: R=0.378 ($p<0.001$); PSMA: R=0.413 ($p<0.001$)].

The interplay between epithelial transcriptomic markers—EpCAM and KRT19—and several parameters including baseline PSA concentrations, CTC#, and prostate cancer-associated transcriptomic genes was explored. To start, correlations between EpCAM and KRT19 with baseline PSA concentrations were exclusively potent in the mCRPC stage as detailed in Figures 6(a) and 6(b) [EpCAM: R=0.476 ($p<0.001$); KRT19: R=0.399 ($p<0.001$)]. Subsequently, a more expansive trend surfaced when assessing relationships between these epithelial genes and CTC# across mHSPC [EpCAM: R=0.462 ($p<0.001$); KRT19: R=0.387 ($p=0.007$)] and mCRPC stages [EpCAM: R=0.508

Preprints (www.preprints.org) | NOT PEER-REVIEWED | Posted: 27 October 2023 doi:10.20944/preprints202310.1760.v1

(p<0.001); KRT19: R=0.296 (p=0.007)] (Figures 6(c) and 6(d)). When correlations between these epithelial genes and mPSA-mRNA were appraised, mHSPC stages exhibited moderate correlations [EpCAM: R=0.466 (p<0.001); KRT19: R=0.526 (p<0.001)] as presented in Figure 6(e), whereas mCRPC stages amplified these correlations as represented in Figure 6(f) [EpCAM: R=0.574 (p<0.001); KRT19: R=0.596 (p<0.001)]. Conclusively, when juxtaposing the epithelial markers with PSMA-mRNA, analogous patterns as those observed with mPSA-mRNA were evident, showcased in Figures 6(g) and 6(h).

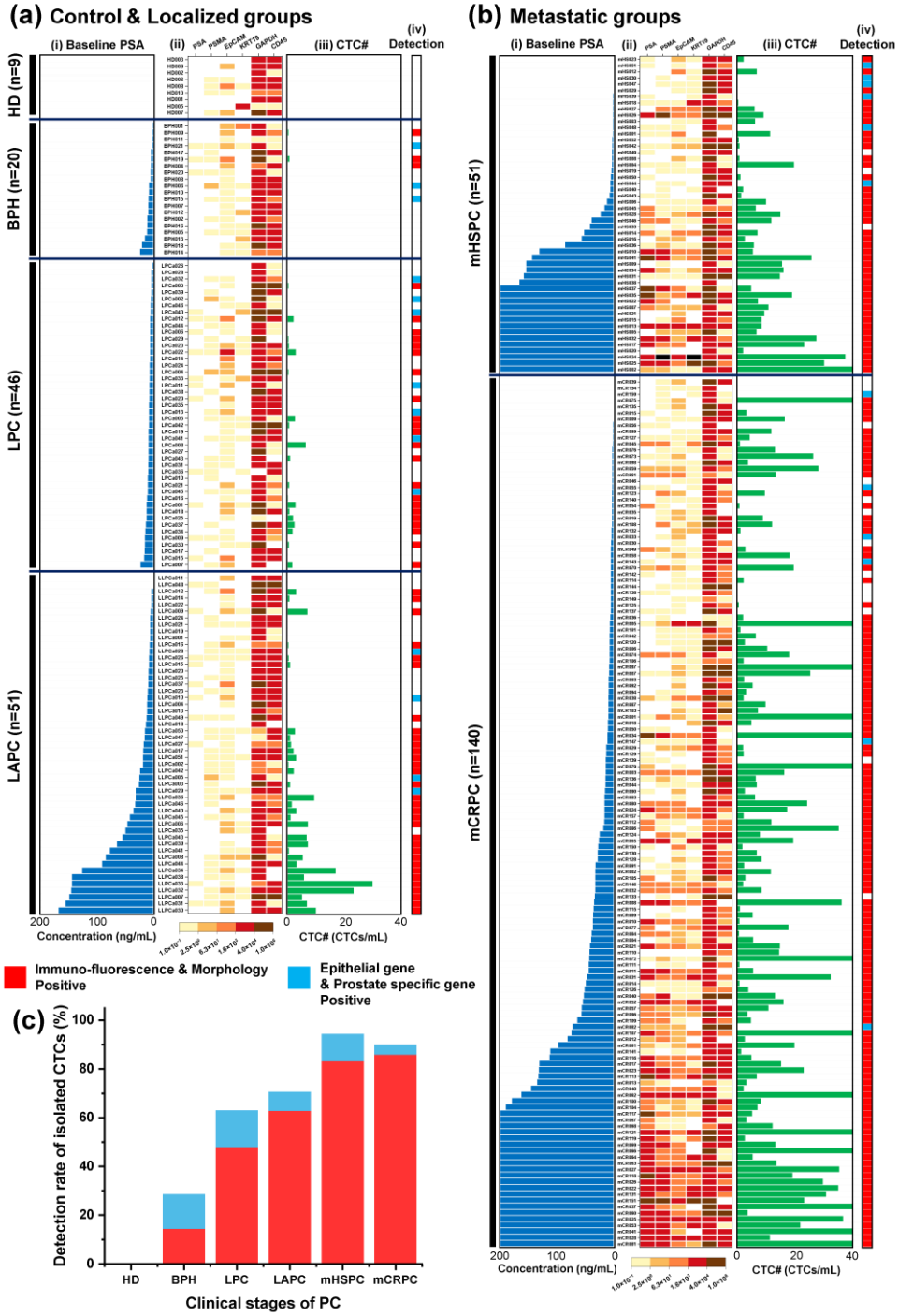

Figure 5. The analysis of CTC detection using numerical and transcriptomic analyses. (a) (i) Baseline PSA, (ii) a heatmap of transcriptomic genes, (iii) CTC#, and (iv) a detection plot of the control, localized, and locally advanced samples are shown (numerical positive in red, transcriptomic positive in blue). (b) (i) Baseline PSA, (ii) a heatmap of transcriptomic genes, (iii) CTC#, and (iv) a detection plot of the metastatic samples are shown (numerical positive in red, transcriptomic positive in blue).

Preprints (www.preprints.org) | NOT PEER-REVIEWED | Posted: 27 October 2023 doi:10.20944/preprints202310.1760.v1

The baseline PSA level is displayed up to a maximum value of 200 ng/mL, and the CTC# is shown up to a maximum of 40 CTCs/mL. (c) The final detection rate of isolated CTCs is analyzed precisely using both numerical and transcriptomic detection.

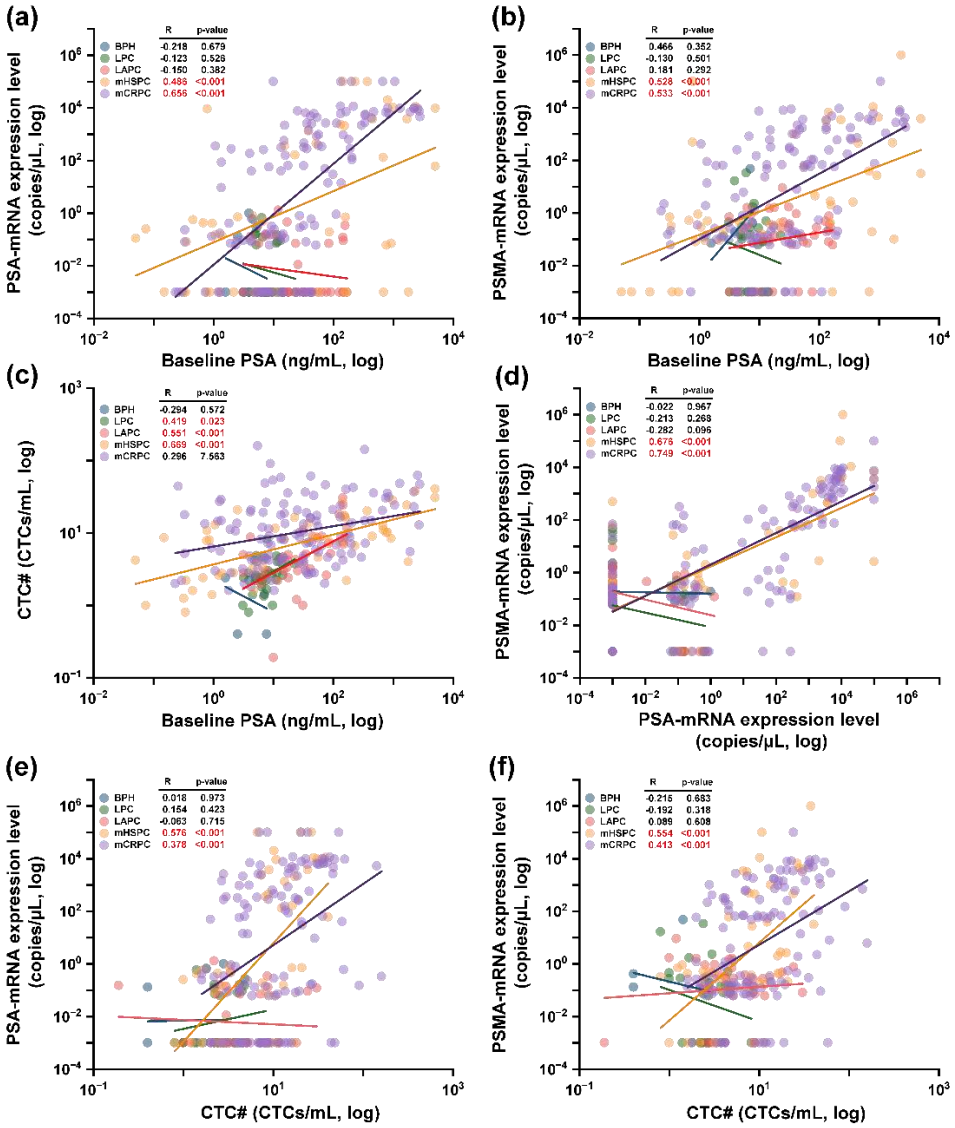

Figure 6. Correlations between CTC#, baseline PSA, PSA-mRNA, and PSMA-mRNA. Each point represents an individual patient sample, categorized by disease stage: BPH, green; LPC, blue; LAPC, yellow; mHSPC, orange; and mCRPC, purple. The trend lines follow the same color scheme. (a) The correlation between baseline PSA levels and PSA-mRNA expression is shown. (b) The correlation between baseline PSA levels and PSMA-mRNA expression is shown. (c) The correlation between PSA-mRNA and PSMA-mRNA levels is shown. (d) The correlation between baseline PSA expression and CTC# is shown. (e) The correlation between CTC# and PSA-mRNA expression is shown. (f) The correlation between CTC# and PSMA-mRNA expression is shown.

Preprints (www.preprints.org) | NOT PEER-REVIEWED | Posted: 27 October 2023 doi:10.20944/preprints202310.1760.v1

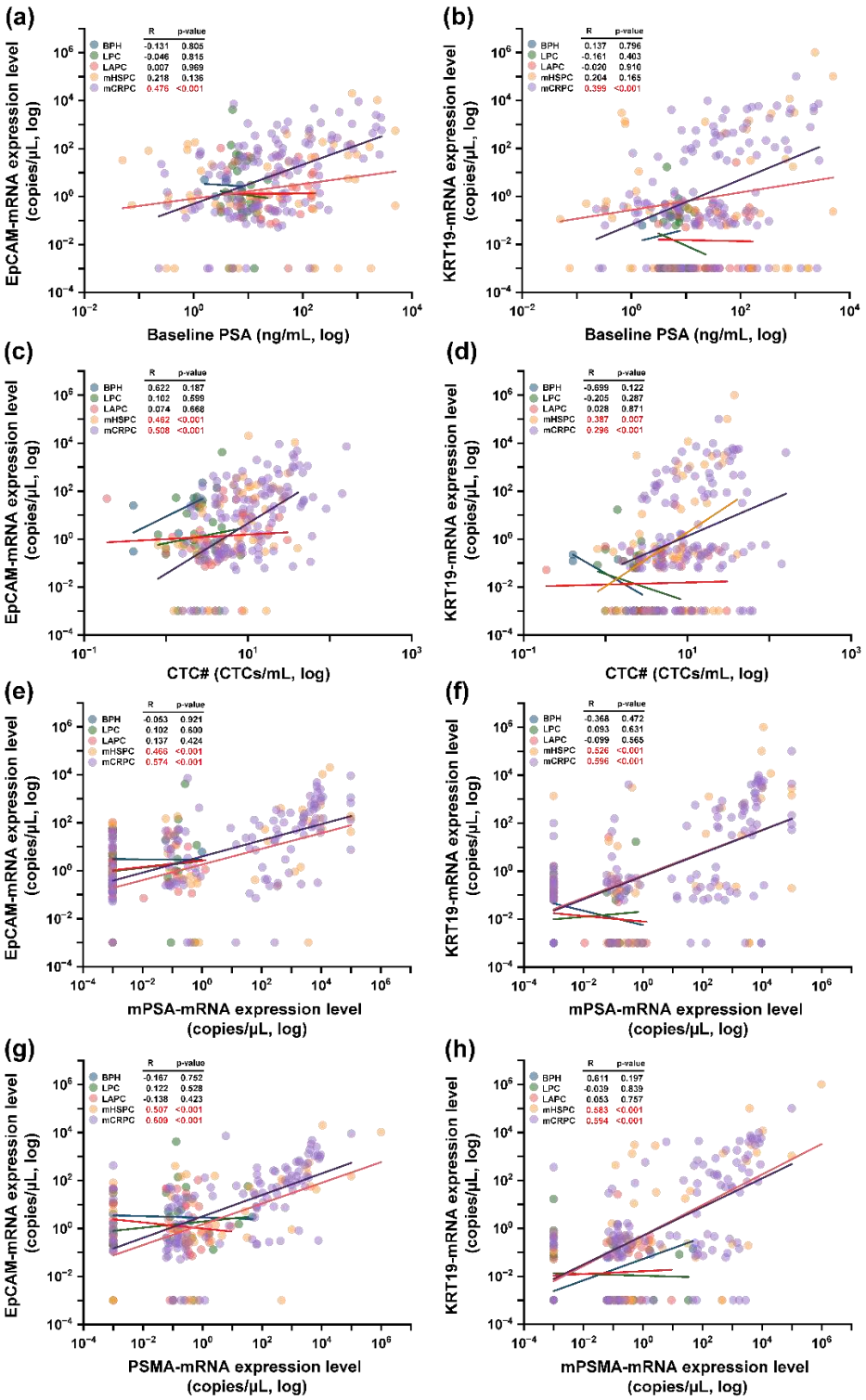

Figure 7. Correlations between CTC#, baseline PSA, PSA-mRNA, PSMA-mRNA, and epithelial transcriptomic genes. Each point represents an individual patient sample, categorized by disease stage: BPH, green; LPC, blue; LAPC, yellow; mHSPC, orange; and mCRPC, purple. The trend lines follow the same color scheme. (a) The correlation between EpCAM-mRNA expression and baseline PSA level is shown. (b) The correlation between KRT19-mRNA expression and baseline PSA level is shown. (c) The correlation between EpCAM-mRNA and expression and CTC# is shown. (d) The correlation between KRT19-mRNA expression and CTC# is shown. (e) The correlation between EpCAM-mRNA expression and PSA-mRNA expression is shown. (f) The correlation between KRT19-mRNA expression and PSA-mRNA expression is shown. (g) The correlation between EpCAM-mRNA

Preprints (www.preprints.org) | NOT PEER-REVIEWED | Posted: 27 October 2023 doi:10.20944/preprints202310.1760.v1

expression and PSMA-mRNA expression is shown. (h) The correlation between KRT19-mRNA expression and PSMA-mRNA is shown.

4. Discussion

Precision medicine is essential for cancer treatment, and the detection and identification of cancer-related biomarkers requires accurate equipment and sensitive gene detection methods. In this study, prostatic CTCs were isolated using microfluidic-based lateral magnetophoresis and transcriptomic gene detection was performed using ddPCR to evaluate the precise detection of CTCs. Then, correlations of CTC data and the clinical stages of PC were analyzed.

As in previous studies [38–40], the CTC# determined using immune-fluorescence and morphology increased as the PC stage progressed from localized to metastatic stage. Traditional microfluidic techniques for isolating CTCs from patients with PC relied on ligands expressed on the cancer cell surface, such as PSMA or EpCAM, and were predominantly used for to determine the metastatic stage, though the detection rate was low for localized PC. Furthermore, commercially-available technologies such as the AdnaTest, which is currently used for CTC isolation and analysis, does not allow for the quantification of CTCs [30]. Traditional quantification methods include transcriptomic PSA, PSMA, and EGFR-based techniques. In this study, a more precise CTC separation and detection technique for patients with PC including the integration of the conventional immuno-fluorescence and morphological approach with the analysis of four transcriptomic genes is presented. This technique resulted in a detection efficiency >60% in localized and advanced localized PC samples and a 20% increase in the detection efficiency compared to that reported in previous our studies [36,37]. The use of gene-based analyses improves the detection efficiency of CTCs by 5-10% compared to conventional immuno-fluorescence and morphological methods. Instead of relying solely on the EpCAM ligand for CTC separation in the blood samples of patients with PC, a more refined CTC isolation method that incorporates an additional set of genes was developed. The combined use of two epithelial-and two prostate-specific genes serves as a foundation for more precise CTC analyses in future studies.

In prostate cancer, the expressions of two PC-specific genes, PSA and PSMA, were correlated with the baseline PSA levels in metastatic PC samples, indicating that these genes derived from CTCs could considered as complementary biological and clinical biomarker with serum PSA concentration. Interestingly, no correlation was observed between baseline PSA and PSA-mRNA and PSMA-mRNA expressions in samples of localized PC, which may be due to lower detection rates and diminished expression levels. These findings highlight the potential of incorporating CTCs and gene detection with conventional PSA analyses as valuable tools for the follow-up of patients with metastatic PC. The CTC# was correlated with baseline PSA in localized PC samples and with mHSPC PC samples. These findings suggest that CTC# can be used as a clinically-meaningful marker for the initial diagnosis of PC and has continued relevance as patients progress from the initial stages of PC to hormone-responsive metastatic stages of PC. No correlation was observed between CTC# and baseline PSA level in the mCRPC samples. Moreover, the epithelial genes EpCAM and KRT19 were correlated with baseline PSA in the mCRPC samples and with CTC# in all metastatic PC samples. Both epithelial genes were also correlated with PSA-mRNA and PSMA-mRNA expressions in the metastatic PC samples. These findings highlight the fact that four genes are overexpressed as the CTC# increases along with their correlation tendency in patients with metastatic PC, suggesting that these four genes could serve as pertinent markers for diagnosing the metastatic stage of PC or as prognostic markers during follow-up. However, minimal expression levels of these genes were detected in localized PC samples.

PSMA, which is overexpressed in patients with recurrent metastatic PC is another potential biomarker. PSMA-PET/CT is currently used to improve the true-positive rate of clinical decisions. Mestre et al. and Minner et al. reported correlations between increased sPSA levels and PSMA PET/CT detection rates [41,42]. Furthermore, PSMA has drawn attention as a target for radionuclides and immunotherapy in patients with mCRPC [43–45]. Therefore, the results of the current study demonstrate that the correlation between PSMA-mRNA and sPSA levels could be used as a

Preprints (www.preprints.org) | NOT PEER-REVIEWED | Posted: 27 October 2023 doi:10.20944/preprints202310.1760.v1

diagnostic marker for PC. The PSA and PSMA genes were strongly correlated with the sPSA levels in the metastatic PC samples in this study (Figure 6d), indicating that the prostate-related genes were actively co-expressed depending on the patient's status, and the combined gene sets may be more precise indicators of a cancer diagnosis or prognosis.

This study has several limitations. First, the CTC assay relied on epithelial expression for the enrichment and identification of CTCs, which may have led to the underestimation of clinically-relevant CTCs undergoing EMT or stem cell-like CTCs. Second, fewer LPC and mHSPC samples were obtained than mCRPC samples. More samples are necessary to obtain more precise and accurate clinical data. Third, more in-depth evaluations using isolated numbers and gene expressions are needed to investigate additional clinical parameters, such as survival probability, biochemical recurrence, and treatment response. However, in this study, the fundamental tendencies of CTC# were determined using more precise methods based on the combination of conventional imaging and transcriptomic analysis that can be applied to other cancer-related investigations.

5. Conclusions

The precise detection and transcriptomic concordance analysis of CTCs from PC using microfluidic-based lateral magnetophoresis and ddPCR offers a promising alternative for PC follow-up biomarker. This study provides valuable insights regarding the limitations of sPSA testing and the potential use of liquid biopsy-based biomarkers for the detection of PC. The results of this study suggest that the precise detection of CTCs using both numerical and transcriptomic analyses can improve the accuracy of PC diagnoses and monitoring techniques. Additionally, PSA-mRNA and PSMA-mRNA derived from CTCs can be used as important markers for PC management. More research is needed to validate these findings and explore the clinical utility of CTC-based liquid biopsies for the management of PC.

Supplementary Materials: The following supporting information can be downloaded at the website of this paper posted on Preprints.org.

Author Contributions: Conceptualization, Hyungseok Cho, Ki-Ho Han and Jae-Seung Chung; Data curation, Hyungseok Cho and Jae-Seung Chung; Formal analysis, Hyungseok Cho, Jae-Seung Chung and Seok-Soo Byun; Funding acquisition, Hyungseok Cho, Ki-Ho Han and Jae-Seung Chung; Investigation, Hyungseok Cho, Ki-Ho Han and Jae-Seung Chung; Methodology, Hyungseok Cho and Ki-Ho Han; Resources, Seok-Soo Byun, Jae Il Chung, Won Ik Seo and Chan Ho Lee; Software, Hyungseok Cho, Jae Il Chung, Won Ik Seo and Chan Ho Lee; Supervision, Ki-Ho Han and Jae-Seung Chung; Validation, Hyungseok Cho, Jae-Seung Chung, Seok-Soo Byun and Jae Il Chung; Visualization, Hyungseok Cho; Writing – original draft, Hyungseok Cho; Writing – review & editing, Ki-Ho Han and Jae-Seung Chung.

Funding: This study was supported by the National Research Foundation of Korea (NRF) and funded by the Korean Government (MSIT) [NRF-2021R1C1C2007117, NRF-2021R1A2C4001594, and NRF-2022R1A2C1002939].

Institutional Review Board Statement: This study was approved by the Institutional Review Boards of Haeundae Paik Hospital (HPIRB 2018-01-005-004) and Seoul National University Bundang Hospital (B-1902-522-304).

Informed Consent Statement: Informed consent was obtained from all subjects involved in the study.

Data Availability Statement: none.

Acknowledgments: none.

Conflicts of Interest: The authors declare no conflict of interest.

Preprints (www.preprints.org) | NOT PEER-REVIEWED | Posted: 27 October 2023 doi:10.20944/preprints202310.1760.v1

References

1. Barry M.J.; Simmons L.H. Prevention of prostate cancer morbidity and mortality: primary prevention and early detection. *Med. Clin. North Am.*; *Medical Clinics* **2017**, *101*, 787-806.
2. Akizhanova M.; Iskakova E.E.; Kim V.; Wang X.; Kogay R.; Turebayeva A.; Sun Q.; Zheng T.; Wu S.; Miao L.; *et al.* PSA and Prostate Health Index based prostate cancer screening in a hereditary migration complicated population: implications in precision diagnosis. *J. Cancer* **2017**, *8*, 1223–1228.
3. Chung J.S.; Morgan T. M.; Hong S.K. Clinical implications of genomic evaluations for prostate cancer risk stratification, screening, and treatment: a narrative review. *Prostate Int.* **2020**, *8*, 99–106.
4. Scher H.I.; Morris M.J.; Basch E.; Heller G. End points and outcomes in castration-resistant prostate cancer: from clinical trials to clinical practice. *J. Clin. Oncol.* **2011**, *29*, 3695–3704.
5. Panteleakou Z.; Lembessis P.; Sourla A.; Pissimissis N.; Polyzos A.; Deliveliotis C.; Koutsilieris M. Detection of circulating tumor cells in prostate cancer patients: methodological pitfalls and clinical relevance. *Mol. Med.* **2009**, *15*, 101-114.
6. Pantel K.; Hille C.; Scher H.I. Circulating tumor cells in prostate cancer: from discovery to clinical utility. *Clin. Chem.* **2019**, *65*, 87-99.
7. Danila D.C.; Heller G.; Gignac G.A.; Gonzalez-Espinoza R.; Anand A.; Tanaka E.; Lilja H.; Schwartz L.; Larson S.; Fleisher M.; *et al.* Circulating tumor cell number and prognosis in progressive castration-resistant prostate cancer. *Clin. Cancer Res.* **2007**, *13*, 7053-7058.
8. Bitting R.L.; Healy P.; Halabi S.; George D.J.; Goodin M.; Armstrong A.J. Clinical phenotypes associated with circulating tumor cell enumeration in metastatic castration–resistant prostate cancer. *Urol. Oncol. Semin. Orig. Investig.* **2015**, *33*, e111-110. e119.
9. Scher H.I.; Curley T.; Geller N.; Engstrom C.; Dershaw D.D.; Lin S.Y.; Fitzpatrick K.; Nisselbaum J.; Schwartz M.; Bezirdjian L. Trimetrexate in prostatic cancer: preliminary observations on the use of prostate-specific antigen and acid phosphatase as a marker in measurable hormone-refractory disease. *J. Clin. Oncol.* **1990**, *8*, 1830-1838.
10. Kallioniemi O.P.; Visakorpi T. Genetic basis and clonal evolution of human prostate cancer. *Adv. Cancer Res.* **1996**, *68*, 225-255.
11. Mejean A.; Vona G.; Nalpas B.; Damotte D.; Brousse N.; Chretien Y.; Dufour B.; Lacour B.; Bréchot C.; Paterlini-Bréchot P. Detection of circulating prostate derived cells in patients with prostate adenocarcinoma is an independent risk factor for tumor recurrence. *J. Urol.* **2000**, *163*, 2022-2029.
12. Pinzani P.; Lind K.; Malentacchi F.; Nesi G.; Salvianti F.; Villari D.; Kubista M.; Pazzagli M.; Orlando C. Prostate-specific antigen mRNA and protein levels in laser microdissected cells of human prostate measured by real-time reverse transcriptase–quantitative polymerase chain reaction and immuno–quantitative polymerase chain reaction. *Hum. Pathol.* **2008**, *39*, 1474-1482.
13. Maas M.; Hegemann M.; Rausch S.; Bedke J.; Stenzl A.; Todenhöfer T. Circulating tumor cells and their role in prostate cancer. *Asian J. Androl.* **2017**, *21*, 24–31.
14. Coumans F.A.W.; Doggen C.J.M.; Attard G.; De Bono J.S.; Terstappen L.W.M.M. All circulating EpCAM+ CK+ CD45-objects predict overall survival in castration-resistant prostate cancer. *Ann. Oncol.* **2010**, *21*, 1851-1857.
15. Grisanti S.; Antonelli A.; Buglione M.; Almici C.; Foroni C.; Sodano M.; Triggiani L.; Greco D.; Palumbo C.; Marini M.; *et al.* Analysis of circulating tumor cells in prostate cancer patients at PSA recurrence and review of the literature. *Anticancer Res.* **2016**, *36*, 2975-2981.
16. Okegawa T.; Nutahara K.; Higashihara E. Immunomagnetic quantification of circulating tumor cells as a prognostic factor of androgen deprivation responsiveness in patients with hormone naive metastatic prostate cancer. *J. Urol.* **2008**, *180*, 1342-1347.
17. Thalgott M.; Rack B.; Maurer T.; Souvatzoglou M.; Eiber M.; Kreß V.; Heck M.M.; Andergassen U.; Nawroth R.; Gschwend J.E.; *et al.* Detection of circulating tumor cells in different stages of prostate cancer. *J. Cancer Res. Clin. Oncol.* **2013**, *139*, 755-763.
18. Goodman Jr O.B.; Symanowski J.T.; Loudyi A.; Fink L.M.; Ward D.C.; Vogelzang N.J. Circulating tumor cells as a predictive biomarker in patients with hormone-sensitive prostate cancer. *Clin. Genitourin. Cancer* **2011**, *9*, 31-38.

Preprints (www.preprints.org) | NOT PEER-REVIEWED | Posted: 27 October 2023 doi:10.20944/preprints202310.1760.v1

19. Helo P.; Cronin A.M.; Danila D.C.; Wenske S.; Gonzalez-Espinoza R.; Anand A.; Koscuiszka M.; Väänänen R.M.; Pettersson K.; Chun F.K.; *et al.* Circulating prostate tumor cells detected by reverse transcription-PCR in men with localized or castration-refractory prostate cancer: concordance with CellSearch assay and association with bone metastases and with survival. *Clin. Chem.* **2009**, *55*, 765-773.
20. Tsumura H.; Satoh T.; Ishiyama H.; Tabata K.I.; Takenaka K.; Sekiguchi A.; Nakamura M.; Kitano M.; Hayakawa K.; Iwamura M. Perioperative search for circulating tumor cells in patients undergoing prostate brachytherapy for clinically nonmetastatic prostate cancer. *Int. J. Mol. Sci.* **2017**, *18*, 128.
21. Khurana K.K.; Grane R.; Borden E.C.; Klein E.A. Prevalence of circulating tumor cells in localized prostate cancer. *Curr. Urol.* **2013**, *7*, 65-69.
22. Bianco Jr F.J.; Powell I.J.; Cher M.L.; Wood Jr D.P. Presence of circulating prostate cancer cells in African American males adversely affects survival. *Urol. Oncol.* **2002**, *7*, 147-152.
23. Shariat S.F.; Gottenger E.; Nguyen C.; Song W.; Kattan M.W.; Andenoro J.; Wheeler T.M.; Spencer D.M.; Slawin K.M. Preoperative blood reverse transcriptase-PCR assays for prostate-specific antigen and human glandular kallikrein for prediction of prostate cancer progression after radical prostatectomy. *Cancer Res.* **2002**, *62*, 5974-5979.
24. Sourla A.; Lembessis P.; Mitsiades C.; Dimopoulos T.; Skouteris M.; Metsinis M.; Ntounis A.; Ioannidis A.; Katsoulis A.; Kyragiannis V.; *et al.* Conversion of nested reverse-transcriptase polymerase chain reaction from positive to negative status at peripheral blood during androgen ablation therapy is associated with long progression-free survival in stage D2 prostate cancer patients. *Anticancer Res.* **2001**, *21*, 3565-3570.
25. Thomas J.; Gupta M.; Grasso Y.; Reddy C.A.; Heston W.D.; Zippe C.; Dreicer R.; Kupelian P.A.; Brainard J.; Levin H.S.; *et al.* Preoperative combined nested reverse transcriptase polymerase chain reaction for prostate-specific antigen and prostate-specific membrane antigen does not correlate with pathologic stage or biochemical failure in patients with localized prostate cancer undergoing radical prostatectomy. *J. Clin. Oncol.* **2002**, *20*, 3213-3218.
26. Joung J.Y.; Cho K.S.; Kim J.E.; Seo H.K.; Chung J.; Park W.S.; Choi M.K.; Lee K.H. Prostate stem cell antigen mRNA in peripheral blood as a potential predictor of biochemical recurrence in high-risk prostate cancer. *J. Surg. Oncol.* **2010**, *101*, 145-148.
27. De Souza M.F.; Kuasne H.; Barros-Filho M.C.; Cilião H.L.; Marchi F.A.; Fuganti P.E.; Rogatto S.R.; Cólus I.M.S. Circulating mRNA signature as a marker for high-risk prostate cancer. *Carcinogenesis* **2020**, *41*, 139-145.
28. Pfitzenmaier J.; Ellis W.J.; Hawley S.; Arfman E.W.; Klein J.R.; Lange P.H.; Vessella R.L. The detection and isolation of viable prostate-specific antigen positive epithelial cells by enrichment: a comparison to standard prostate-specific antigen reverse transcriptase polymerase chain reaction and its clinical relevance in prostate cancer. *Urol. Oncol.* **2007**, *25*, 214-220.
29. Russo G.I.; Bier S.; Hennenlotter J.; Beger G.; Pavlenco L.; van de Flierdt J.; Hauch S.; Maas M.; Walz S.; Rausch S.; *et al.* Expression of tumour progression-associated genes in circulating tumour cells of patients at different stages of prostate cancer. *BJU Int.* **2018**, *122*, 152-159.
30. Cho H.; Chung J.S.; Han K.H. A direct comparison between the lateral magnetophoretic microseparator and AdnaTest for isolating prostate circulating tumor cells. *Micromachines* **2020**, *11*, 870.
31. Broncy L.; Paterlini-Bréchot P. Clinical impact of circulating tumor cells in patients with localized prostate cancer. *Cells* **2019**, *8*, 676.
32. Doyen J.; Alix-Panabières C.; Hofman P.; Parks S.K.; Chamorey E.; Naman H.; Hannoun-Lévi J.M. Circulating tumor cells in prostate cancer: a potential surrogate marker of survival. *Crit. Rev. Oncol. Hematol.* **2012**, *81*, 241-256.
33. Cho H.; Kim J.; Jeon C.W.; Han K.H. A disposable microfluidic device with a reusable magnetophoretic functional substrate for isolation of circulating tumor cells. *Lab Chip* **2017**, *17*, 4113-4123.
34. Cha J.; Cho H.; Chung J.S.; Park J.S.; Han K.H. Effective circulating tumor cell isolation using epithelial and mesenchymal markers in prostate and pancreatic cancer patients. *Cancers* **2023**, *15*, 2825.
35. Kim J.; Cho H.; Kim J.; Park J.S.; Han K.H. A disposable smart microfluidic platform integrated with on-chip flow sensors. *Biosens. Bioelectron.* **2021**, *176*, 112897.
36. Cho H.; Chung J.I.; Kim J.; Seo W.I.; Lee C.H.; Morgan T.M.; Byun S.S.; Chung J.S.; Han K.H. Multigene model for predicting metastatic prostate cancer using circulating tumor cells by microfluidic magnetophoresis. *Cancer Sci.* **2021**, *112*, 859-870.

Preprints (www.preprints.org) | NOT PEER-REVIEWED | Posted: 27 October 2023 doi:10.20944/preprints202310.1760.v1

37. Cho H.; Oh C.K.; Cha J.; Chung J.I.; Byun S.S.; Hong S.K.; Chung J.S.; Han K.H. Association of serum prostate-specific antigen (PSA) level and circulating tumor cell-based PSA mRNA in prostate cancer. *Prostate Int.* **2022**, *10*, 14-20.
38. Kalfazade N.; Kuskucu A.M.; Karadag S.; Sahin S.; Aras B.; Midilli K.; Yılmaz G.; Tasci A.I. nephrology. Quantification of PSA mRNA levels in peripheral blood of patients with localized prostate adenocarcinoma before, during, and after radical prostatectomy by quantitative real-time PCR (qRT-PCR). *Int. Urol.* **2009**, *41*, 273-279.
39. Miyamoto D.T.; Lee R.J.; Kalinich M.; LiCausi J.A.; Zheng Y.; Chen T.; Milner J.D.; Emmons E.; Ho U.; Broderick K.; *et al.* An RNA-based digital circulating tumor cell signature is predictive of drug response and early dissemination in prostate cancer. *Cancer Discov.* **2018**, *8*, 288-303.
40. Theil G.; Boehm C.; Fischer K.; Bialek J.; Hoda R.; Weber E.; Schönburg S.; Kawan F.; Fornara P. In vivo isolation of circulating tumor cells in patients with different stages of prostate cancer. *Oncol. Lett.* **2021**, *21*, 357.
41. Minner S.; Wittmer C.; Graefen M.; Salomon G.; Steuber T.; Haese A.; Huland H.; Bokemeyer C.; Yekebas E.; Dierlamm J.; *et al.* High level PSMA expression is associated with early PSA recurrence in surgically treated prostate cancer. *Prostate* **2011**, *71*, 281-288.
42. Pereira Mestre R.; Treglia G.; Ferrari M.; Pascale M.; Mazzara C.; Azinwi N.C.; Llado', A.; Stathis, A.; Giovanella, L.; Roggero, E. Correlation between PSA kinetics and PSMA-PET in prostate cancer restaging: a meta-analysis. *European journal of clinical investigation* **2019**, *49*, e13063.
43. Kratochwil C.; Giesel F.L.; Stefanova M.; Benešová M.; Bronzel M.; Afshar-Oromieh A.; Mier W.; Eder M.; Kopka K.; Haberkorn U. PSMA-targeted radionuclide therapy of metastatic castration-resistant prostate cancer with 177Lu-labeled PSMA-617. *J. Nucl. Med.* **2016**, *57*, 1170-1176.
44. Lamb A.D.; Bryant R.J.; Mills I.G.; Hamdy F.C. First report of prostate-specific membrane antigen-targeted immunotherapy in prostate cancer: the future is bright. *Eur. Urol.* **2018**, *73*, 653–655.
45. Zhang Q.; Helfand B.T.; Carneiro B.A.; Qin W.; Yang X.J.; Lee C.; Zhang W.; Giles F.J.; Cristofanilli M.; Kuzel T.M. Efficacy against human prostate cancer by prostate-specific membrane antigen-specific, transforming growth factor-β insensitive genetically targeted CD8+ T-cells derived from patients with metastatic castrate-resistant disease. *Eur. Urol.* **2018**, *73*, 648-652.

Disclaimer/Publisher's Note: The statements, opinions and data contained in all publications are solely those of the individual author(s) and contributor(s) and not of MDPI and/or the editor(s). MDPI and/or the editor(s) disclaim responsibility for any injury to people or property resulting from any ideas, methods, instructions or products referred to in the content.